A LETTERS JOURNAL EXPLORING
THE FRONTIERS OF PHYSICS

OFFPRINT

Enhancing mammalian hearing by a balancing between spontaneous otoacoustic emissions and spatial coupling

ZONGHUA LIU, BAOWEN LI and YING-CHENG LAI

EPL, **98** (2012) 20005

Please visit the new website
www.epljournal.org

epl

A Letters Journal Exploring the Frontiers of Physics

AN INVITATION TO SUBMIT YOUR WORK

www.epljournal.org

The Editorial Board invites you to submit your letters to EPL

EPL is a leading international journal publishing original, high-quality Letters in all areas of physics, ranging from condensed matter topics and interdisciplinary research to astrophysics, geophysics, plasma and fusion sciences, including those with application potential.

The high profile of the journal combined with the excellent scientific quality of the articles continue to ensure EPL is an essential resource for its worldwide audience. EPL offers authors global visibility and a great opportunity to share their work with others across the whole of the physics community.

Run by active scientists, for scientists

EPL is reviewed by scientists for scientists, to serve and support the international scientific community. The Editorial Board is a team of active research scientists with an expert understanding of the needs of both authors and researchers.

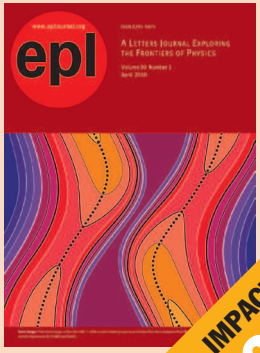

IMPACT FACTOR 2.753*

*As ranked by ISI 2010

IMPACT FACTOR
2.753*
* As listed in the ISI® 2010 Science Citation Index Journal Citation Reports

OVER
500 000
full text downloads in 2010

30 DAYS
average receipt to online publication in 2010

16 961
citations in 2010
37% increase from 2007

"We've had a very positive experience with EPL, and not only on this occasion. The fact that one can identify an appropriate editor, and the editor is an active scientist in the field, makes a huge difference."

Dr. Ivar Martinv
Los Alamos National Laboratory, USA

Six good reasons to publish with EPL

We want to work with you to help gain recognition for your high-quality work through worldwide visibility and high citations.

1. **Quality** – The 40+ Co-Editors, who are experts in their fields, oversee the entire peer-review process, from selection of the referees to making all final acceptance decisions
2. **Impact Factor** – The 2010 Impact Factor is 2.753; your work will be in the right place to be cited by your peers
3. **Speed of processing** – We aim to provide you with a quick and efficient service; the median time from acceptance to online publication is 30 days
4. **High visibility** – All articles are free to read for 30 days from online publication date
5. **International reach** – Over 2,000 institutions have access to EPL, enabling your work to be read by your peers in 100 countries
6. **Open Access** – Articles are offered open access for a one-off author payment

Details on preparing, submitting and tracking the progress of your manuscript from submission to acceptance are available on the EPL submission website **www.epletters.net**.

If you would like further information about our author service or EPL in general, please visit **www.epljournal.org** or e-mail us at **info@epljournal.org**.

EPL is published in partnership with:

European Physical Society | Società Italiana di Fisica | EDP Sciences | IOP Publishing

epl

A Letters Journal
Exploring the Frontiers
of Physics

EPL Compilation Index

www.epljournal.org

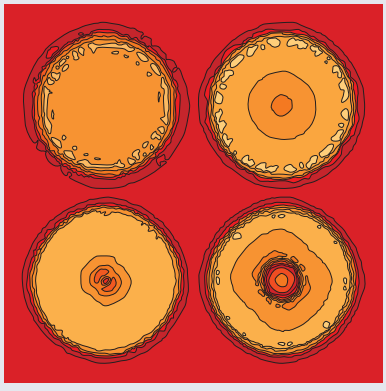

Biaxial strain on lens-shaped quantum rings of different inner radii, adapted from **Zhang *et al*** 2008 EPL **83** 67004.

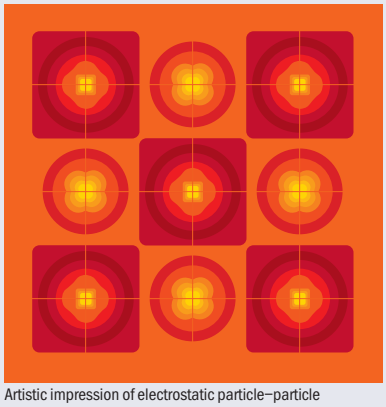

Artistic impression of electrostatic particle–particle interactions in dielectrophoresis, adapted from **N Aubry and P Singh** 2006 *EPL* **74** 623.

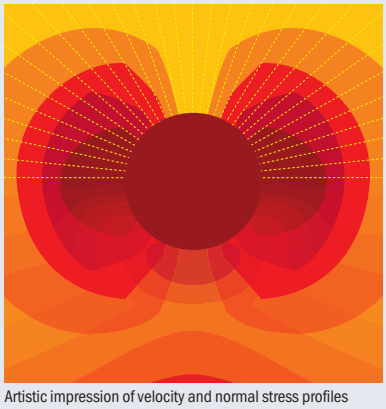

Artistic impression of velocity and normal stress profiles around a sphere that moves through a polymer solution, adapted from **R Tuinier, J K G Dhont and T-H Fan** 2006 *EPL* **75** 929.

Visit the EPL website to read the latest articles published in cutting-edge fields of research from across the whole of physics.

Each compilation is led by its own Co-Editor, who is a leading scientist in that field, and who is responsible for overseeing the review process, selecting referees and making publication decisions for every manuscript.

- Graphene
- Liquid Crystals
- High Transition Temperature Superconductors
- Quantum Information Processing & Communication
- Biological & Soft Matter Physics
- Atomic, Molecular & Optical Physics
- Bose–Einstein Condensates & Ultracold Gases
- Metamaterials, Nanostructures & Magnetic Materials
- Mathematical Methods
- Physics of Gases, Plasmas & Electric Fields
- High Energy Nuclear Physics

If you are working on research in any of these areas, the Co-Editors would be delighted to receive your submission. Articles should be submitted via the automated manuscript system at **www.epletters.net**

If you would like further information about our author service or EPL in general, please visit **www.epljournal.org** or e-mail us at **info@epljournal.org**

EPS Società Italiana di Fisica EDP SCIENCES **IOP** Publishing

Image: Ornamental multiplication of space-time figures of temperature transformation rules (adapted from T. S. Bíró and P. Ván 2010 *EPL* **89** 30001; artistic impression by Frédérique Swist).

A Letters Journal Exploring the Frontiers of Physics

April 2012

EPL, **98** (2012) 20005
doi: 10.1209/0295-5075/98/20005

www.epljournal.org

Enhancing mammalian hearing by a balancing between spontaneous otoacoustic emissions and spatial coupling

Zonghua Liu[1,2(a)], Baowen Li[2,3] and Ying-Cheng Lai[4,2]

[1] *Institute of Theoretical Physics and Department of Physics, East China Normal University 200062, Shanghai, China*
[2] *Department of Physics and Centre for Computational Science and Engineering, National University of Singapore 117546, Singapore*
[3] *Centre for Phononics and Thermal Energy Science, Department of Physics, Tongji University 200092, Shanghai, China*
[4] *School of Electrical, Computer and Energy Engineering, Arizona State University - Tempe, AZ 85287, USA*

received 13 February 2012; accepted in final form 26 March 2012
published online 30 April 2012

PACS 05.45.-a – Nonlinear dynamics and chaos
PACS 87.19.lt – Sensory systems: visual, auditory, tactile, taste, and olfaction
PACS 87.10.Ca – Analytical theories

Abstract – Nonlinear dynamics has provided significant insights into the origin of frequency discrimination and signal amplification underlying mammalian hearing. Existing signal amplification models, however, tend to ignore two basic known aspects of the hearing: spontaneous otoacoustic emissions (SOAEs) and intrinsic dynamical coupling in the cochlea. We construct and study a class of coupled-oscillator models to remedy this deficiency. Our analysis and computations reveal that the interplay and balance between the two aspects can naturally explain the phenomena of frequency discrimination and signal amplification and, more strikingly, the origin of hearing loss, all at a quantitative level. In the presence of SOAEs, there exists a critical coupling threshold below which hearing loss can occur, suggesting enhancement of coupling as a potentially effective therapeutic strategy to restore or even significantly enhance hearing.

Copyright © EPLA, 2012

We live in a world of sound and our abilities to hear and to discriminate sound are a result of natural evolution and are essential to the quality of life. There is a long history of research on the mechanism and sensitivity of mammalian hearing [1] but a complete understanding is still lacking, rendering necessary interdisciplinary efforts among physics, physiology, and biomedical engineering. It is now understood that frequency discrimination and signal amplification are realized in the inner ear called the cochlea, which has the shape of a snail and coils about two and half rounds. An acoustic signal in the audible frequency range, when propagating into the cochlea, can excite a traveling wave along the basilar membrane (BM), whose amplitude reaches a peak at a position that depends on the frequency of the signal. This gives rise to the frequency discrimination ability, where the amplitude peak position varies from high frequency at the base of the cochlea to low frequency at the apex [2,3]. Signal amplification, however, can be attributed to some physical mechanism that actively generates energy in the ear. Key to realizing frequency discrimination and signal amplification is the organ of Corti that consists of three rows of outer hair cells and a single row of inner hair cells, the former being responsible for enhancing the BM motion while the latter translating sound-induced mechanical stimuli into a neurotransmitter signal to the auditory nerve [1,4–6]. To understand the fundamental physics and physiology underlying the phenomena of frequency discrimination and signal amplification, various artificial electronic realizations of the cochlea have been investigated [7–11].

It has been realized that the signal amplification in the inner ear is an active process in which the spontaneous otoacoustic emissions (SOAEs), weak acoustic oscillations in a broad frequency range, take a key role. SOAEs have been discovered and studied for more than three decades [12–15]. It is suggested that SOAEs are some kinds of standing waves created by multiple internal reflections and can be triggered by two ways [16–18]. One

(a) E-mail: zhliu@phy.ecnu.edu.cn

supposes that SOAEs are passive biological noise, while the other supposes that SOAEs are actively maintained by coherent wave amplification within the cochlea. The stimulus frequency emission provides an important non-diagnostic tool to test the cochlear functions, especially for newborn babies. SOAEs can be also understood by a class of coupled-oscillator models [19–21], where the coupling is rooted in the observation that the outer hair cells of the mammalian cochlea are directly linked via their hair bundles to the elastic tectorial membrane [6,22,23] and thus result in finite coupling with their neighbors. An interesting result is that the coupling may induce frequency clustering in SOAEs.

Recent years have witnessed an increasing appreciation for the use of nonlinear dynamics to probe into the fundamentals of mammalian hearing [10,12,21–31]. These efforts suggested that the active amplifier of the cochlea may be understood as a dynamical system about to undergo a Hopf bifurcation so that it would be sensitive to stimuli at the frequency generated by the bifurcation. The existing models usually focus on a parameter region before the Hopf bifurcation and use an isolated oscillator to study the signal amplification. Thus, they have not taken into account two known aspects associated with hearing: 1) SOAEs and 2) interactions among different segments of the BM. These two aspects are, however, fundamental to mammalian hearing. From the standpoint of dynamics, SOAEs were identified to be limit-cycle oscillations [32,33]. This, however, generates a paradox with respect to current understanding of the frequency sensitivity, because limit-cycle oscillations are typically found in dynamical systems slightly past the Hopf bifurcation point. The second aspect comes from the coupling mechanism of SOAEs [19–21]. Furthermore, the necessity to consider coupling lies in the fact that the number of hair cells in the human cochlea decays throughout life as a result of genetic abnormalities, ear infections, loud sounds, ototoxic drugs, and aging etc. [34,35]. As a result, hearing loss may be regarded as a dynamical manifestation of the decrease in the coupling strength among different oscillators constituting the cochlea.

In this letter, we present a coupled-oscillators model to address the effects of both SOAEs and spatial coupling on the dynamics of hearing. In particular, the cochlea is modeled as an array of coupled nonlinear oscillators. To generate spontaneous oscillations, each oscillator is assumed to be slightly post Hopf bifurcation. The coupling strength can be decreased to model hearing loss. Our model is thus more comprehensive than any previous ones in the field of nonlinear dynamics of hearing. The appealing feature is that our model can explain the phenomena of frequency discrimination and signal amplification in a natural and unified manner, without any contradiction. In particular, the two phenomena can result from a balance between the depth of the system into Hopf bifurcation and the coupling strength among the oscillators. The significance is that, in the presence of spatial coupling, frequency

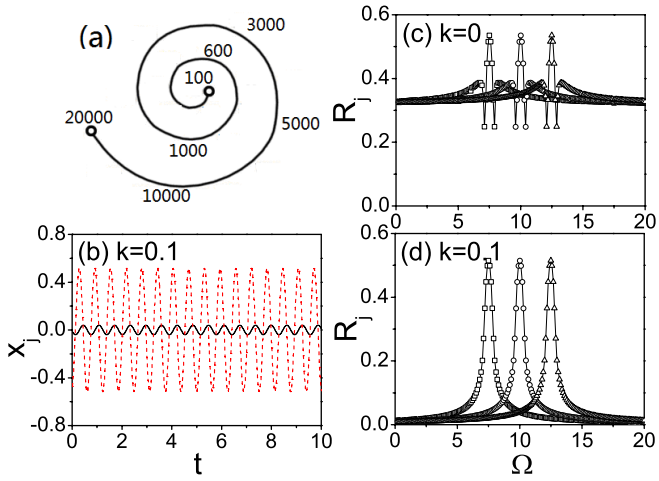

Fig. 1: (Color online) (a) Schematic illustration of frequency distribution in the cochlea where the numbers represent the characteristic frequencies at different points along the BM; (b) for a stimulated signal with amplitude $f = 0.1$ and frequency $\Omega = 10$, time series $x_j(t)$ at two positions of the BM with $\omega_j = 7.5$ (solid curve) and $\omega_j = 10$ (dashed curve); (c) R_j *vs.* Ω for $k = 0$; and (d) R_j *vs.* Ω for $k = 0.1$. In panels (b)–(d), the parameter μ is fixed at $\mu = 0.1$.

sensitivity can be achieved even when the system is in a post Hopf bifurcation state, in contrast to results from the existing dynamical models. We also find that signal amplification can be characterized by a power law with varying exponents, depending on how far the system is from the critical bifurcation point. A striking result is that, at a quantitative level, spatial coupling plays a fundamental role in shaping the hearing ability: hearing loss can occur when the coupling is below a critical threshold. This in turn suggests that, as a potentially effective therapeutic strategy, hearing may be significantly enhanced by strengthening the coupling. Our study indicates that, to obtain a deeper and more complete understanding of mammalian hearing, it is necessary to probe into the spatiotemporal dynamics of coupled nonlinear oscillators. While the oscillator model that we employ is idealized, we choose the parameters so that it captures the essential features of mammalian hearing dynamics. Our model represents a new paradigm to understand the fundamental dynamics of mammalian hearing based on spatiotemporal dynamics, the latter itself being an active area of research in nonlinear science.

Our coupled-array model is constructed, as follows. We assume that the cochlea is a one-dimensional chain of N serially connected oscillators. Each oscillator has the characteristic frequency ω_j, where $\omega_i < \omega_j$ for $i < j$, as shown schematically in fig. 1(a). Following previous works [10,24–27], we choose the oscillator such that its dynamics naturally exhibits a Hopf bifurcation. One such choice is $\dot{z} = (\mu + i\omega_0)z - |z|^2 z$, where $z(t)$ is a complex variable of time, ω_0 is the natural frequency of oscillation, and μ is the bifurcation parameter. Our model can thus

be written as

$$\dot{z}_j = (\mu + i\omega_j)z_j - |z_j|^2 z_j + k(z_{j+1} + z_{j-1} - 2z_j) + fe^{i\Omega t}, \quad (1)$$

for $j = 1, \ldots, N$, where k is the coupling strength, ω_j is the characteristic frequency of oscillator j, and $fe^{i\Omega t}$ is an acoustic signal of amplitude f and frequency Ω. When $f = 0$, eq. (1) is similar to the coupling oscillator model of SOAEs [20]. We here focus on the case of $f > 0$ and pay attention to how signal is amplified, in contrast to focus on the features of SOAEs such as the frequency clustering in ref. [20]. For the case of $k = 0$ and $f = 0$, the solution of eq. (1) is $z_j = \sqrt{\mu}e^{i\omega_j t}$. Thus, $\mu = 0$ is the critical point, where limit-cycle oscillations occur for $\mu > 0$ and there is a fixed point for $\mu < 0$. For the case of $k > 0$ and $f > 0$, however, the solutions of eq. (1) are completely different. There are in fact two distinct cases.

Category I. For oscillators whose characteristic frequencies ω_j are close to the external frequency Ω, we may assume a $1:1$ frequency-locked solution of the form $z_j = R_j e^{i(\Omega t - \lambda x + \phi)}$, where λ is the wave number. Substituting this expression into eq. (1), we obtain

$$f^2 = R_j^2[(R_j^2 + k\lambda^2 - \mu)^2 + (\Omega - \omega_j)^2], \quad (2)$$

which is cubic in R_j^2. When the coupling satisfies approximately the condition $k\lambda^2 - \mu \simeq 0$, we can simplify eq. (2) as

$$f^2 = R_j^2[R_j^4 + (\Omega - \omega_j)^2], \quad (3)$$

whose solution is given by

$$3R_j^2 = \left(\frac{27f^2 + D}{2}\right)^{1/3} + \left(\frac{27f^2 - D}{2}\right)^{1/3}, \quad (4)$$

where $D = \sqrt{(27f^2)^2 + 4(3(\Omega - \omega_j)^2)^3}$. For $\omega_j = \Omega$ we have

$$R_j = f^{1/3}. \quad (5)$$

The solution in the low signal frequency regime is not as straightforward. Qualitatively, for fixed f, k and μ, we see from eq. (2) that R_j decreases monotonously with the term $(\Omega - \omega_j)^2$.

Depending on the coupling strength, there are three cases: $k\lambda^2 - \mu < 0$, $k\lambda^2 - \mu = 0$, and $k\lambda^2 - \mu > 0$. Letting $k_c \equiv \mu/\lambda^2$ be the critical coupling strength, the three cases correspond to $k < k_c$, $k = k_c$, and $k > k_c$, respectively. For the first case of $k < k_c$, we focus on the situation of $\omega_j = \Omega$. For $f \ll 1$, the solution of eq. (2) can be explicitly obtained as $R_j^2 - (\mu - k\lambda^2) \approx f$, which results in

$$R_j \approx \mu - k\lambda^2 + f \approx \mu - k\lambda^2. \quad (6)$$

That is, approximately, R_j is independent of f. For the second case of $k = k_c$, eq. (2) is identical to eq. (3) so the relationship between R_j and f for $\omega_j = \Omega$ is also given by eq. (5). This relationship coincides with the corresponding relation at the bifurcation point $\mu = 0$ from previous models in the absence of spatial coupling [10,25–27]. For the third case of $k > k_c$, we may approximately treat R_j^2 as a small quantity and thus obtain the solution of eq. (2) as

$$R_j \approx f/\sqrt{(k\lambda^2 - \mu)^2 + (\Omega - \omega_j)^2} \sim f. \quad (7)$$

That is, R_j is linearly proportional to f. Comparing with eq. (2), eq. (7) indicates explicitly that R_j will reach its maximal value at $\Omega = \omega_j$ and then monotonously decrease with the increase in the frequency difference $|\Omega - \omega_j|$.

The above discussion can also be extended to the case of $\mu = 0$, which corresponds to $k_c = 0$. In this situation, we will not have the first case of $k < k_c$ but only the second and third cases.

Category II. For those oscillators whose characteristic frequencies ω_j are far from the external frequency Ω, we may assume a solution of the form $z_j = z_1' + z_2' = r_1 e^{i(\Omega t - \lambda x + \phi_1)} + r_2 e^{i(\omega_j t + \phi_2)} \equiv Re^{i(\omega' t + \phi)}$, where $R = r_1^2 + r_2^2 + 2r_1 r_2 \cos(\omega_j t + \phi_2 - \Omega t - \phi_1 + \lambda x)$. Substituting this into eq. (1), we obtain

$$\begin{aligned} i\Omega z_1' + i\omega_j z_2' \;=\; & (\mu + i\omega_j)(z_1' + z_2') \\ & -(R^2 + k\lambda^2)(z_1' + z_2') + fe^{i\Omega t}. \end{aligned} \quad (8)$$

A specific solution of eq. (8) can be obtained by letting

$$\begin{aligned} i\omega_j z_2' &= (\mu + i\omega_j)z_2' - (R^2 + k\lambda^2)z_2', \\ i\Omega z_1' &= (\mu + i\omega_j)z_1' - (R^2 + k\lambda^2)z_1' + fe^{i\Omega t} \end{aligned} \quad (9)$$

which gives

$$R = \sqrt{\mu - k\lambda^2}, \quad (10)$$

$r_1^2 = f^2/(\Omega - \omega_j)^2 \to 0$ and $r_2 \to \sqrt{\mu - k\lambda^2}$. Thus, the solution is

$$z_j = \sqrt{\mu - k\lambda^2}e^{i(\omega_j t + \phi_2)}, \quad (11)$$

which vanishes for $k > k_c$, indicating that the effect of coupling will completely suppress that of SOAEs.

From the above analysis, we see that, for a given signal, the response R_j will reach its maximum at the location on the BM for which $\omega_j = \Omega$ holds and then gradually decrease as the point moves away from this location. For locations whose ω_j values are different from Ω, the values of R_j are insignificant. That is, for a given external frequency, only a small, localized region of the BM is responsive, providing the BM with the necessary frequency discrimination capability. We also note that, a convenient quantity to characterize signal amplification is R_j/f [10,25,26], whose frequency scaling obeys a power law with exponent -1 for $k < k_c$, $-2/3$ for the critical coupling k_c, and 0 for $k > k_c$.

We now provide numerical support for our theoretical predictions. For concreteness, we set $\mu = 0.1$ and $N = 101$. For clear presentation of results, we normalize the audible frequency range [100, 20000] into an arbitrary range [5, 15] and let ω_i be uniformly distributed in this range with $\omega_1 = 5$ and $\omega_N = 15$, as shown in fig. 1(a). We then project the frequency of the external acoustic signal into the range

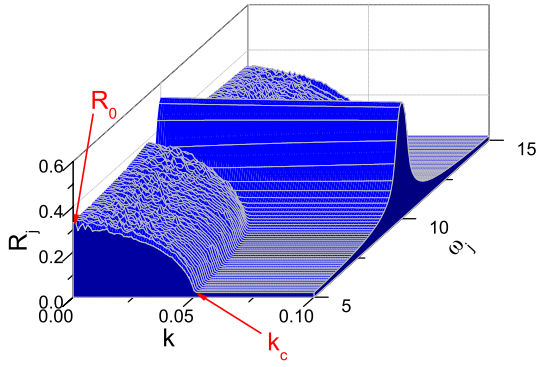

Fig. 2: (Color online) For $\mu = 0.1$ and $\Omega = 10$, R_j *vs.* k and ω_j, where k_c denotes the critical coupling strength given by $\mu = k_c\lambda^2$ and R_0 represents the value of R_j at those points with $k = 0$ and ω_j values markedly different from Ω.

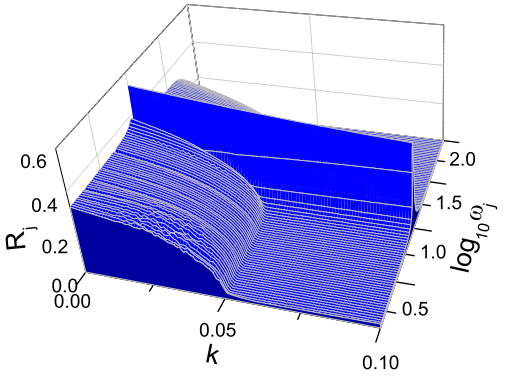

Fig. 3: (Color online) For $\mu = 0.1$ and $\Omega = 10$, R_j *vs.* k and ω_j, where the frequency ω_j is not uniformly but logarithmic distributed in $[0, 2]$, *i.e.*, $\omega_j \in (1, 100]$.

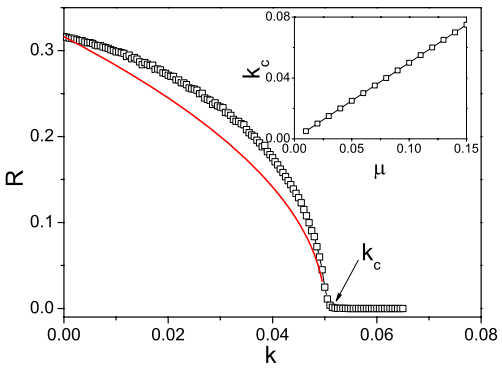

Fig. 4: (Color online) Numerically calculated behavior of R *vs.* k (squares) as compared with the theoretical prediction eq. (10) (solid line). Shown in the inset is the critical coupling strength k_c *vs.* μ.

$[0.1, 20]$, *i.e.*, $\Omega \in [0.1, 20]$, where the subranges $[0.1, 5)$ and $(15, 20]$ correspond to inaudible sound signals. We let $z_j = x_j + iy_j$ in eq. (1) and calculate the evolution of x_j. Figure 1(b) shows how x_j changes with time t at two typical points for $k = 0.1$ and $f = 0.1$. We see that the difference between the amplitudes of the two curves is large, indicating different degrees of sensitivity to external signal. To characterize this sensitivity, we let R_j be the time average of the maximum of x_j, *i.e.*, $R_j = \langle \max(x_j) \rangle$, change the frequency Ω of the external signal systematically from 0.1 to 20, and then calculate the values of R_j at three representative positions with $\omega_j = 7.5, 10$, and 12.5, respectively. Figures 1(c) and (d) show the variations of R_j with Ω at these positions for the cases of $k = 0$ and $k = 0.1$, respectively. Comparing figs. 1(c) with (d), we see that the background R_j in fig. 1(c) is much larger than that in fig. 1(d), indicating stronger resonances in R_j at all three characteristic frequencies in fig. 1(d). These results thus suggest that the coupling among neighboring segments in the cochlea plays a key role in its frequency discrimination capability.

To see how spatial coupling counterbalances the effect of positive μ, we consider a specific signal with frequency $\Omega = 10$. We set $\mu = 0.1$ and increase k systematically from 0 to 0.1. We find that, for the points whose ω_j values are not far away from Ω, the corresponding values of R_j decrease monotonously with $|\Omega - \omega_j|$, confirming our theoretical prediction eqs. (2) and (7), as can be seen by the appearance of a hump in the central region of fig. 2. We also see that, for the points whose ω_j values are different from Ω, the corresponding values of R_j apparently do not depend on $|\Omega - \omega_j|$ but decrease from R_0 to 0 as k is increased from 0 to $k = k_c$, as shown in fig. 2.

While we have considered uniform frequency distribution, the behavior of R_j *vs.* k and ω_j is robust with respect to alternative frequency distributions. For example, recognizing that the range of the audible frequency is quite large, we have considered a logarithmic distribution. Figure 3 shows the result where the frequency ω_j is distributed logarithmically in the interval $(1, 100]$, with other parameters the same as in fig. 2. Comparing figs. 3 with 2, we see that they exhibit essentially the same features.

The dependence of R_j on k can be predicted, as follows. Notice that, for frequency ω_j sufficiently different from Ω, the corresponding value of R_j is exactly the value of any R_j when there is no external signal. We are thus led to calculate the dependence of R_j on k for the case of no signal, as shown by the "square" curve in fig. 4. This dependence can, however, also be calculated directly from formula (10), as shown by the solid line in fig. 4. We observe a reasonable agreement, validating eq. (10). Furthermore, by definition k_c is proportional to μ, which is also confirmed numerically, as shown in the inset of fig. 4.

An important prediction of our coupled-array model concerns about the influences of the balance between μ and k on signal amplification, as predicted by eqs. (2) and (7). To provide numerical support, we first consider the case of $\mu = 0$. Since $k_c = 0$, it suffices to choose several values of k in the $k > k_c$ regime. For each chosen value of k, we let the signal amplitude f increase from 10^{-5} to 10^{-1} and calculate the response R_j. Figure 5(a) shows the results

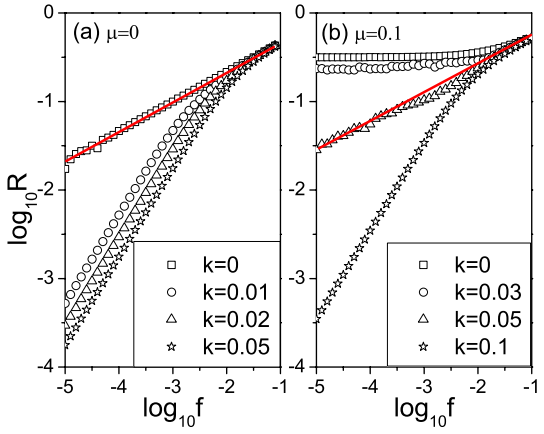

Fig. 5: (Color online) (a) For $\mu = 0$, power-law scaling between R_j and f for $k = 0$ (squares), $k = 0.01$ (circles), $k = 0.02$ (triangles), and $k = 0.05$ (stars). (b) For $\mu = 0.1$, the corresponding scaling for $k = 0$ (squares), $k = 0.03$ (circles), $k = 0.05$ (triangles), and $k = 0.1$ (stars).

for $k = 0$, 0.01, 0.02 and 0.05. In all cases, a power-law scaling relation is observed. However, for $k = 0$, the scaling exponent is 1/3 for the whole frequency range considered, while for other cases, the same exponent is observed only for $f > 10^{-2}$ and, for $f < 10^{-2}$, the scaling exponent is actually 1. These results agree with the theoretical prediction of eqs. (5) and (7) very well.

We then consider the case of $\mu > 0$. Take $\mu = 0.1$ as an example. From the inset of fig. 4, we obtain $k_c = 0.05$ and can then test all three cases: $k < k_c$, $k = k_c$ and $k > k_c$. Representative results are shown in fig. 5(b), where we observe a universal scaling exponent for all cases in the frequency range $f > 10^{-2}$, confirming eq. (5). For $f < 10^{-2}$, there are three cases: i) for $k < k_c$, the value of R_j is approximately constant; ii) for $k = k_c$, there is a power-law scaling with the scaling exponent 1/3, and i)–ii) for $k > k_c$, the scaling exponent is 1. The results from the three cases also agree very well with the theoretical predictions of eqs. (6), (5), and (7), respectively. Moreover, both figs. 5(a) and (b) show that there is a scaling exponent 1/3 at the balance point k_c. This result agrees with the cochlea experimental data where the response to external force is demonstrated to obey a power law with exponent approximately 0.4 [12,36].

The constant curves in fig. 5(b) have the following physiological meaning. The impairment of hair cells due to aging can effectively reduce the coupling strength to below the threshold k_c. As a result, SOAEs cannot be completely suppressed (see fig. 2), leading to an insensitivity to weak signal and henceforth hearing loss. For $k > k_c$, the scaling exponent 1 in figs. 5(a) and (b) implies that the cochlea is more sensitive to weak signal than the normal cochlea with the scaling exponent 1/3, regardless of the presence of SOAEs. Dynamically, superior hearing can then result from strong coupling between neighboring segments of the BM. This observation suggests a potential therapeutic method for improving hearing: increasing the internal dynamical coupling within the cochlea.

In summary, we have developed a coupled-oscillator model to study the effect of SOAEs and spatial coupling on frequency discrimination and signal amplification of the cochlea. Theoretical analysis and numerical computations identify the internal coupling strength as key to hearing. There exists a critical coupling strength, below which hearing loss can occur but above which a high degree of hearing sensitivity can be achieved in terms of frequency discrimination and signal amplification. This has potentially important implications to developing effective treatment for hearing loss. Our work represents another example where principles and methods of nonlinear dynamics may be used to understand physiological systems and to develop novel therapeutic strategies to improve human health.

* * *

This work was partially supported by the NNSF of China under Grant Nos. 10975053 and 11135001 (ZL), and by ONR under Grant No. N00014-08-1-0627 (Y-CL).

REFERENCES

[1] See, for example, Pickles J. O., *An Introduction to the Physiology of Hearing*, 2nd edition (Academic Press) 1988.
[2] Olson E. S., *J. Acoust. Soc. Am.*, **115** (2004) 1230.
[3] Dallos P., *J. Neurosci.*, **12** (1992) 4575.
[4] Narayan S. S., Temchin A. N. and Recio A. *et al.*, *Science*, **282** (1998) 1882.
[5] Nilsen K. E. and Russell I. J., *Proc. Natl. Acad. Sci. U.S.A.*, **97** (2000) 11751.
[6] Ashmore J. F., Geleoc G. S. G. and Harbott L., *Proc. Natl. Acad. Sci. U.S.A.*, **97** (2000) 11759.
[7] Martignoli S., van der Vyver J.-J., Kern A., Uwate Y. and Stoop R., *Appl. Phys. Lett.*, **91** (2007) 064108.
[8] Martin P., Hudspeth A. J. and Julicher F., *Proc. Natl. Acad. Sci. U.S.A.*, **98** (2001) 14380.
[9] Martin P. and Hudspeth A. J., *Proc. Natl. Acad. Sci. U.S.A.*, **98** (2001) 14386.
[10] Kern A. and Stoop R., *Phys. Rev. Lett.*, **91** (2003) 128101.
[11] Hubbard A., *Science*, **259** (1993) 68.
[12] Camalet S., Duke T., Julicher F. and Prost J., *Proc. Natl. Acad. Sci. U.S.A.*, **97** (2000) 3183.
[13] Kemp D. T., *J. Acoust. Soc. Am.*, **64** (1978) 1386.
[14] Nobili R., Vetesnik A., Turicchia L. and Mammano F., *JARO*, **4** (2003) 478.
[15] Probst R., Lonsbury-Martin B. L. and Martin G. K., *J. Acoust. Soc. Am.*, **89** (1991) 2027.
[16] Zweig G. and Shera C. A., *J. Acoust. Soc. Am.*, **98** (1995) 2018.
[17] Shera C. A. and Guinan J. J., *J. Acoust. Soc. Am.*, **105** (1999) 782.
[18] Shera C. A., *J. Acoust. Soc. Am.*, **114** (2003) 244.

[19] Duifhuis H., Hoogstraten H. W., van Netten S. M., Diependaal R. J. and Bialek W., *Modelling the cochlear partition with coupled Van der Pol oscillators*, in *Peripheral Auditory Mechanisms*, edited by Allen J. B., Hall J. L., Hubbard A. E., Neely S. T. and Tubis A. (Springer, New York) 1985, pp. 290–297.
[20] Vilfan A. and Duke T., *Biophys. J.*, **95** (2008) 4622.
[21] Barral J., Dierkes K., Lindner B., Julicher F. and Martin P., *Proc. Natl. Acad. Sci. U.S.A.*, **107** (2010) 8079.
[22] Prakash R. and Ricci A. J., *Proc. Natl. Acad. Sci. U.S.A.*, **105** (2008) 18651.
[23] Dierkes K., Lindner B. and Julicher F., *Proc. Natl. Acad. Sci. U.S.A.*, **105** (2008) 18669.
[24] Risler T., Prost J. and Julicher F., *Phys. Rev. Lett.*, **93** (2004) 175702.
[25] Eguiluz V. M., Ospeck M., Choe Y., Hudspeth A. J. and Magnasco M. O., *Phys. Rev. Lett.*, **84** (2000) 5232.
[26] Stoop R. and Kern A., *Phys. Rev. Lett.*, **93** (2004) 268103.
[27] Montgomery K. A., Silber M. and Solla S. A., *Phys. Rev. E*, **75** (2007) 051924.
[28] Magnasco M. O., *Phys. Rev. Lett.*, **90** (2003) 058101.
[29] Duke T. and Julicher F., *Phys. Rev. Lett.*, **90** (2003) 158101.
[30] Martignoli S. and Stoop R., *Phys. Rev. Lett.*, **105** (2010) 048101.
[31] Lamb J. S. and Chadwick R. S., *Phys. Rev. Lett.*, **107** (2011) 088101.
[32] Murphy W. J., Tubis A., Talmadge C. L., Long G. R. and Krieg E. F., *Proc. Natl. Acad. Sci. U.S.A.*, **100** (1996) 3979.
[33] Yates G. K. and Kirk D. L., *J. Neurosci.*, **18** (1998) 1996.
[34] Bruce I. C., Sachs M. B. and Young E. D., *J. Acoust. Soc. Am.*, **113** (2003) 369.
[35] Hudspeth A. J. and Konishi M., *Proc. Natl. Acad. Sci. U.S.A.*, **97** (2000) 11690.
[36] Ruggero M. A., Rich N. C., Narayan S. S. and Robles L., *J. Acoust. Soc. Am.*, **101** (1997) 2151.